

## Investigation of Acoustic and Vibrational Properties Using Laser Doppler Vibrometry (LDV) and Electronic Speckle Pattern Interferometry (ESPI) of the Kulintangan Instruments

Sinin Hamdan<sup>1\*</sup>, Ahmad Faudzi Musib<sup>2</sup>, Khairul Anwar Mohamad Said<sup>1</sup>,  
Saiful Hairi Othman<sup>3</sup> and Marini Sawawi<sup>1</sup>

<sup>1</sup>Faculty of Engineering, Universiti Malaysia Sarawak, 94300 UNIMAS, Kota Samarahan, Sarawak, Malaysia

<sup>2</sup>Faculty of Human Ecology, Universiti Putra Malaysia, 43400 UPM, Serdang, Selangor, Malaysia

<sup>3</sup>Institute of Creative Arts and Technology, Universiti Malaysia Sarawak, 94300 UNIMAS, Kota Samarahan, Sarawak, Malaysia

### ABSTRACT

This study visualises the mode of the vibration of kulintangan using Electronic Speckle Pattern Interferometry (ESPI) to reveal the modes. It was found that the production of sound by the kulintangan was dominated by a particular mode which may be the (0,1), (1,1), (2,2), (3,2), and (4,2) of free edge circular gong. The spectrum distribution from the strike on the kulintangan showed it. The small gong A-H has an approximately harmonic spectrum with a fundamental frequency of 1240, 1055, 934, 792, 705, 624, 474, and 422 Hz. The gong does not display a similar occurrence of harmonics due to the ruggedness of the surface texture of the gong. This finding can be of great importance to facilitate a better understanding of the mechanisms involved in the sound production of musical instruments. Our research is visualising the sound sonically through PicoScope oscilloscopes and ESPI.

*Keywords:* Acoustic, Electronic Speckle Pattern Interferometry (ESPI), Laser Doppler Vibrometry (LDV), vibrations

### ARTICLE INFO

*Article history:*

Received: 22 April 2022

Accepted: 16 August 2022

Published: 20 March 2023

DOI: <https://doi.org/10.47836/pjst.31.2.24>

*E-mail addresses:*

hsinin@unimas.my (Sinin Hamdan)

faudzimusib@upm.edu.my (Ahmad Faudzi Musib)

miskanwar@unimas.my (Khairul Anwar Mohamad Said)

hosaiful@unimas.my (Saiful Hairi Othman)

smarini@unimas.my (Marini Sawawi)

\* Corresponding author

### INTRODUCTION

Visualising structural vibrations is important to understand acoustics. Two hundred years ago, Ernst Chladni introduced a common technique by placing sand on a vibrating flat plate for imaging the vibrations. Over the last 50 years, inexpensive methods to help students visualise vibrational mode shapes are still not widely available. Scanning Laser

Doppler Vibrometry (LDV) is an effective method for visualising steady-state structural vibrations, which costs several hundred thousand dollars. Electronic speckle pattern interferometry (ESPI) is one method of visualising structural deflection shapes that are widely used for research and can be used in an educational setting.

A kulintangan is a traditional musical instrument from the general region of Sabah Malaysia. The backbone of the kulintangan consists of gongs of various sizes with a similar general form and made of iron. The kulintangan is central to the musical art of Sabah, which commands huge respect and reverence. Scanning Laser Doppler Vibrometry (LDV) and electronic speckle pattern interferometry (ESPI) are used together with acoustical measurements.

The data validity from tone measurements of idiophones (particularly gongs) was questionable by Schneider (2001). Normal modes of a small gamelan gong using ESPI and finite element methods were done by Perrin et al. (2014) and Herington et al. (2010). Finite element analysis and gong acoustics were done by McLachlan (1997). The spectral analysis of tones produced on such instruments does not show clear, obvious ‘fundamental,’ but an inharmonic spectrum that yields auditory uncertainty. The data generated by tone-measuring equipment produced erroneous results. Bronze is the favoured and most expensive material of construction for gongs. Bronze instruments produce a richer tone, i.e., more appealing than iron instruments. Iron instruments, especially iron gongs, are much easier to tune than bronze counterparts. Figure 1 shows the vibrational modes of circular plates (a) free edge and (b) clamped or simply supported edge (Fletcher & Rossing, 1999). From Figure 1, the symbol  $(m, n)$  is used where ‘ $m$ ’ is the nodal diameter, whereas ‘ $n$ ’ is the nodal circle of the node produced from the vibration.  $(3,0)$  means 3 nodal diameters and 0 nodal circles. The sound from musical instruments is strongly related to their vibrational mode, and Raman (1934) first reported the viewing technique. The main objective of this study was to gain a better understanding of how kulintangan vibrates when it is struck. It can be achieved partially by first investigating the mode of its vibration.

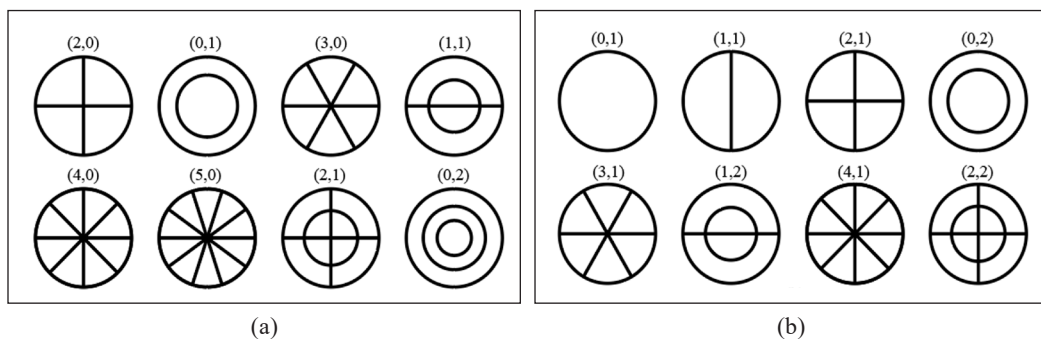


Figure 1. Vibrational modes of circular plates: (a) free edge and (b) clamped or simply supported edge [Fletcher and Rossing, 1999]

Kulintangan is a traditional musical instrument of the Kadazan Dusun, Bajau, Brunei Malay, and other ethnic groups in Sabah. A set of kulintangan consists of 8 to 12 small gongs (Alman, 1961) or 7 to 9 (Frame 1976). This work investigates 8 small steel gongs (label A to H) and a big steel gong. This work explored both the acoustical and vibrational aspects of the gongs. Previous measurements on the kulintangan frequency using the Fourier transform were done by Dusin (2001), whereas the physical characteristics, i.e., the correlation between the diameter and frequency, were done by Batahong and Dayou (2001). Dayou (2002) found that the sound from a good-quality kulintangan should consist of a single frequency for each gong.

The pitch of an iron gong can be increased or decreased by cold hammering (with little risk of permanent damage). Bronze gongs' pitch can be altered by hammering (which could result in cracking) or by scraping (permanently removes metal and reduces a tuner's options for future pitch adjustments). The approach to tuning an iron gong differs from that of a bronze gong. The pitch is lowered by cold hammering the flat surface around the knob of an iron gong from the top. The pitch can be raised by hammering the same surface inside the iron gong.

## MATERIAL AND METHODS

A set of kulintangan consisting of 8 small iron gongs was used in this research. This work reports a typical small iron gong from Sabah with a diameter of <20cm. The dimension of the gong varies in the diameter where the rim and the thickness are consistent except for gongs A and H. The rim length for all gongs is 38mm except gong A and gong H, i.e., 34 and 43 mm, respectively. The diameter for the gongs increased gradually from A (17 cm), B (17.6 cm), C (17.8 cm), D (17.8 cm), E (18.2 cm), F (19 cm), G (20 cm) to H (18.6 cm). The thickness of the gongs ranges between 1.66 to 1.72 mm. This work reported gong G with a diameter of 20 cm. The resonance testing was conducted for all the gongs. Figure 2 shows one of the typical small iron gongs. The gongs were bought from the street market at Kundasang, Sabah, Malaysia. Most sound analyses and re-synthesis of the gong are investigating the tone systems. This work measured the fundamental frequency, harmonics, and sub-harmonics using Fourier transformation. The different intensities and harmonics or sub-harmonics (overtones) differentiate individual gong characters. Most importantly, this work showed the range of available frequencies at a specific time. Our study was conducted on a series of small iron gongs with a diameter of less



Figure 2. A typical small iron gong

than 20 cm. All the gongs sit on two pieces of stretch string and simulate the real situation when played.

### Microphone Method

Figure 3 shows the experimental setup for the microphone method. An expert player struck the gong. The microphone was held above the top surface of the gong along the axis of symmetry at a distance of about 20 cm.

In this study, the audio signal derived from the striking by an expert player (an experienced gamelan ensemble player with a musical ear and knowledge of musical notation) is recorded. The audio signal is recorded in mono, at 24-bit resolution and 48 kHz sampling rate. The audio signal is recorded with a digital interface in a “.wav” format.

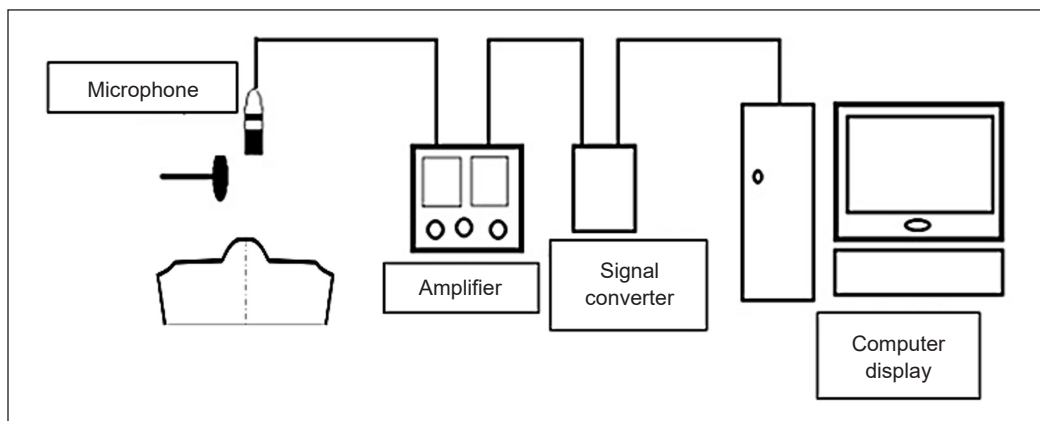


Figure 3. Schematic diagram of the experimental setups for the microphone method.

Audio signal calibration of the recording system is carried out to ensure the recorded audio signal is at the optimum level. A 1 kHz sine wave test tone calibrates the recording system. Here the ‘unity’ calibration level is at +4 dBu or -10 dBV and is read by the recording device at ‘0 VU’. In this regard, the European Broadcast Union (EBU) recommended that the digital equivalent of 0VU is that the test tone generated by the recording device of the experimentation is recorded at -18 dBFS (Digital) or +4 dBu (Analog), which is equivalent to 0VU. EBU defines the calibration standard for all manufactured professional audio recording devices and replay units. In this thorough calibration procedure, no devices unknowingly boost or attenuate its amplitude in the signal chain when the recording is carried out. The recording apparatus was the Steinberg UR22 mkII audio interface, Audio-Technica AT4050 microphone, XLR cable (balance), with microphone position on axis (<20 cm) and microphone setting with low cut (flat) 0 dB.

The PicoScope computer software (Pico Technology, 3000 series, Eaton Socon, UK) was used to view and analyse the time signals from PicoScope oscilloscopes (Pico

Technology, 3000 series, Eaton Socon, UK) and data loggers for real-time signal acquisition. PicoScope software enables analysis using Fast Fourier transform (FFT), a spectrum analyser, voltage-based triggers, and the ability to save/load waveforms to a disk. The amplifier (Behringer Powerplay Pro XL, Behringer, China) ensured the sound capture was loud enough to be detected by the signal converter.

### **Laser Doppler Vibrometer (LDV)**

Having identified all the possible frequencies obtained through the microphone method, the Laser Doppler Vibrometer (LDV) was conducted to capture the vibration of the Eigen frequency from the gong and reconfirm all the resonance frequencies obtained from the microphone method. To investigate the motion at selected places on the surface of the gong, a Polytec Compact Laser Vibrometer was used to complement the ESPI measurements. The laser sampled an area of about 4 mm<sup>2</sup>, considered as taking point measurements. The vibrometer output was recorded on a PC, and a Fourier transform was performed to determine the frequencies present. In the acoustic case, the vibration is excited by a hard rubber hammer, while in the LDV case, it is excited by the loudspeaker. The gongs were excited acoustically by means of a speaker driven by a signal generator and placed approximately a meter away from the gong. The distance was adjusted to yield the optimum vibrations on the gong to be captured by the LDV. The vibrations of the gong were recorded using the Pico oscilloscope, which can perform Fourier transform. A precautionary measure was taken with regard to the above measurements possibly being made on a nodal section of the gong. If the laser were normally pointed downwards onto a section of the gong's surface acting at a node, then no frequencies relevant to the gong's vibration would be found during the Fourier transform. Six locations were chosen on the surface of the gong, and LDV was undertaken at each point. The points were nominated as points 1-6, with point 1 being at the closest proximity to the knob and with increasing integer labels, the greater the distance from the knob.

Not all the resonance frequencies obtained from the microphone method are shown by the LDV, especially the high frequencies mode, although this is very clear through the microphone method. Since the microphone does not detect a frequency lower than 100 Hz, the LDV had the advantage of detecting the lower frequency by scanning through from 0 to 100 Hz. It appears to be consistent. The small gong was labelled considering its diameter, and the results of the resonance frequencies of each gong are shown as a series where the ordinate of the graph represents the frequency (Hz). At the same time, the abscissa counts a number of resonance frequencies. Figure 4 shows the experiment performed on the gong using non-contact sinusoidal excitation at a frequency close to one Eigen frequency of the gong.

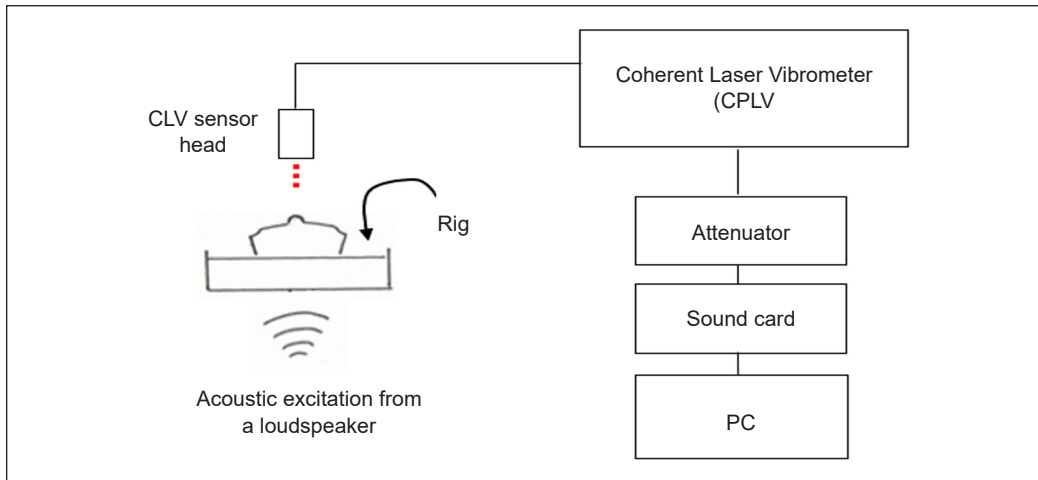


Figure 4. Apparatus setup for non-contact sinusoidal acoustic excitation and non-contact laser detector at specific Eigen frequency

### Electronic Speckle Pattern Interferometry (ESPI)

Having done the microphone method and LDV, the electronic speckle pattern interferometry (ESPI) experiment was conducted on all the small gongs. ESPI is another non-contact technique that allows qualitative measurements of displacement to be made. The investigation analyses the linear modal analysis of the gongs. It makes several comparisons for the whole gongs. ESPI reported several mode patterns of resonance, similar among all the series of gongs. The gong was mounted on a vibration-isolated optical table inside an anechoic chamber driven by a speaker about 50 cm from it. A sinusoidal signal which drove the speaker was produced from a high-quality function generator (to avoid introducing harmonic and subharmonic signals). Unfortunately, the system did not permit the gong to be supported horizontally, as it would be during normal playing. Instead, it was hung vertically, clamped to a stand along a small section near the rim's centre. It would certainly have influenced some of the modes when interpreting the results.

The frequencies explored were in the range of 30 Hz-5 kHz. Images were observed on the computer screen, and when a pattern of deflections of the gong was observed, an image was saved for analysis. It is essential to have some information about the nodal patterns for as many cases as possible, i.e.,  $m$  and  $n$  values, to identify split doublets, harmonics, and subharmonics. The results obtained by the CCD camera were shown on a computer monitor, and screenshots were taken. The frequency of the input signal supplied by the speaker was noted. The gong area placed under the test was perpendicular to the beam of the laser to increase the intensity of the results; the modes are analysed almost exclusively independently.

## RESULTS AND DISCUSSION

### Microphone Method

These investigations started with an experiment using a microphone method on the gongs subjected to a big strike on the dome. When struck by a soft hammer, the spectrum of the sound examined is notable that it evolves significantly over a time of about one second. The initial sound just decayed without any significant partials, as shown in Figures 5 and 6. The dimension of the small gong varies in diameter, where the rim and the thickness are consistent except for gongs A and H. The rim length for all gongs is 38 mm except gong A and gong H, i.e., 34 and 43 mm, respectively. The diameter for the gongs increased

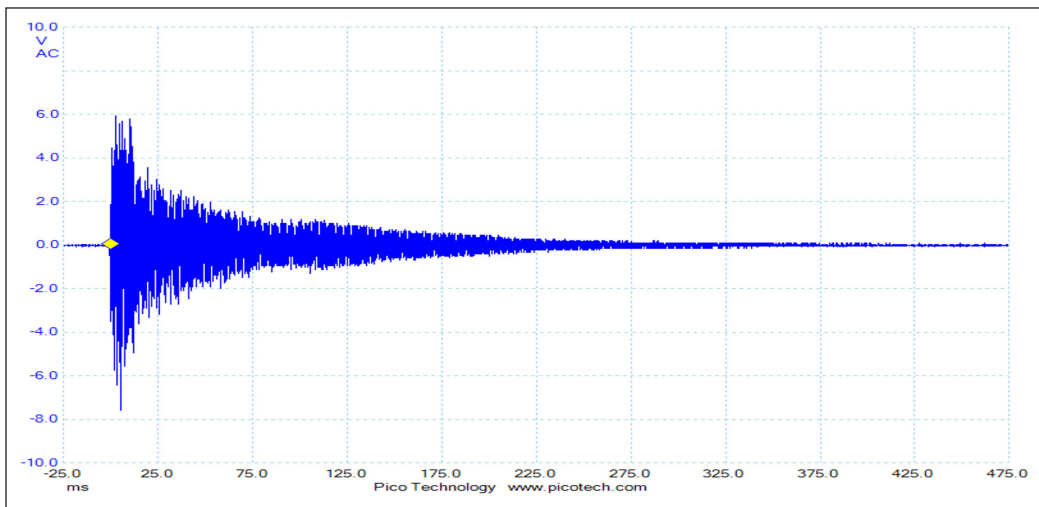


Figure 5: Acoustic signal of a small gong

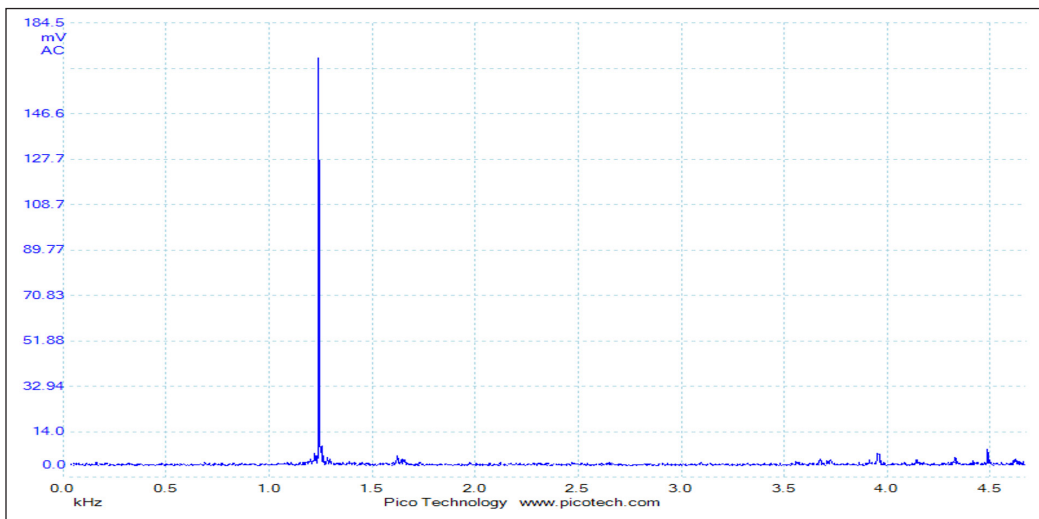
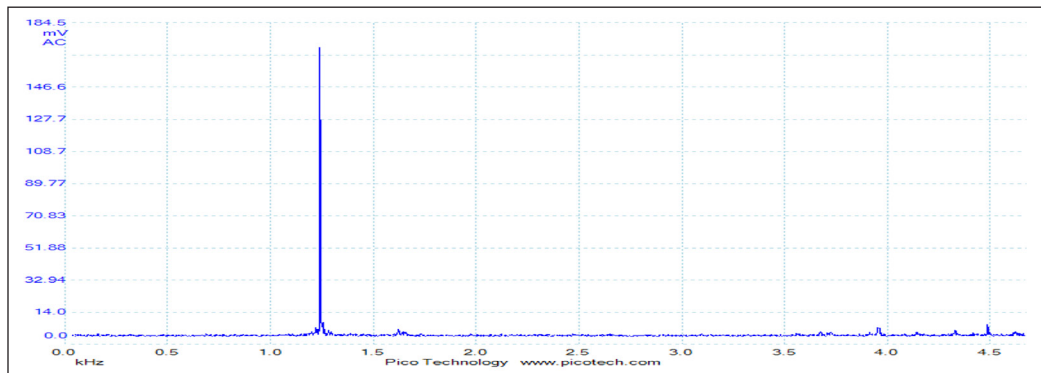


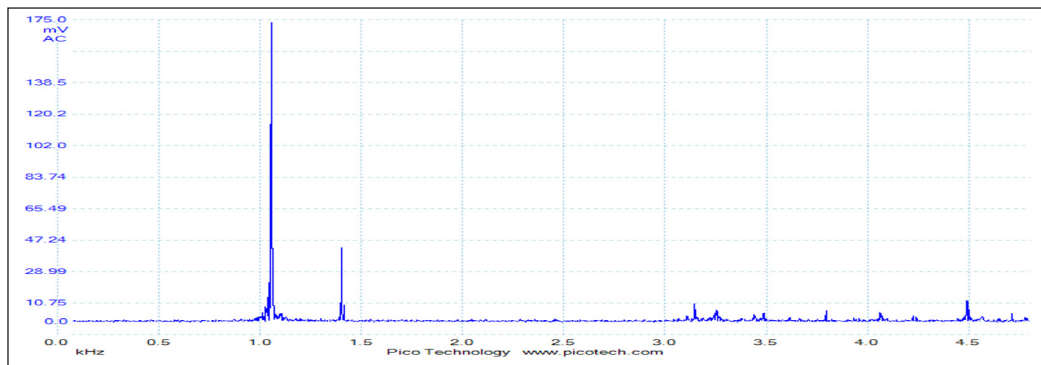
Figure 6. Sound pressure level spectra of a small gong

gradually from A (17 cm), B (17.6 cm), C (17.8 cm), D (17.8 cm), E (18.2 cm), F (19cm), G (20 cm) to H (18.6 cm). The thickness of the gongs ranges between 1.66 to 1.72 mm.

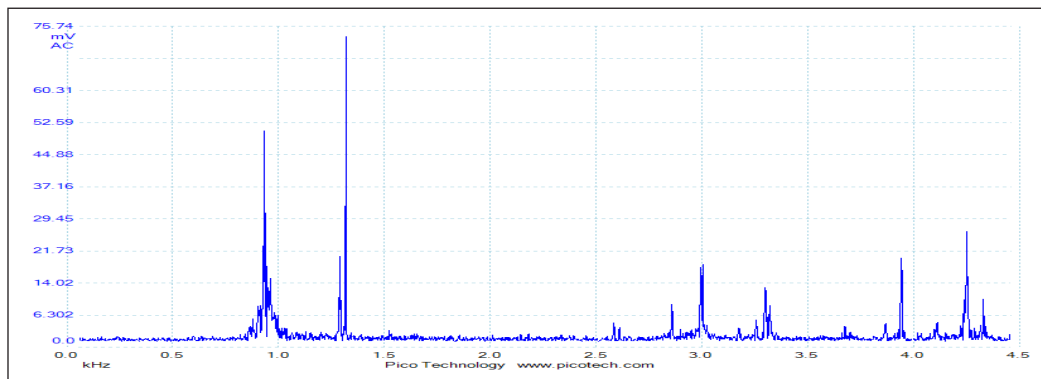
Figure 7 shows the acoustic spectra recorded about 500 milliseconds after excitation of 8 small iron gongs of less than 200 mm diameter. These acoustic spectra agree quite well with the non-contact sinusoidal excitation at a frequency close to one Eigen frequency



(a)



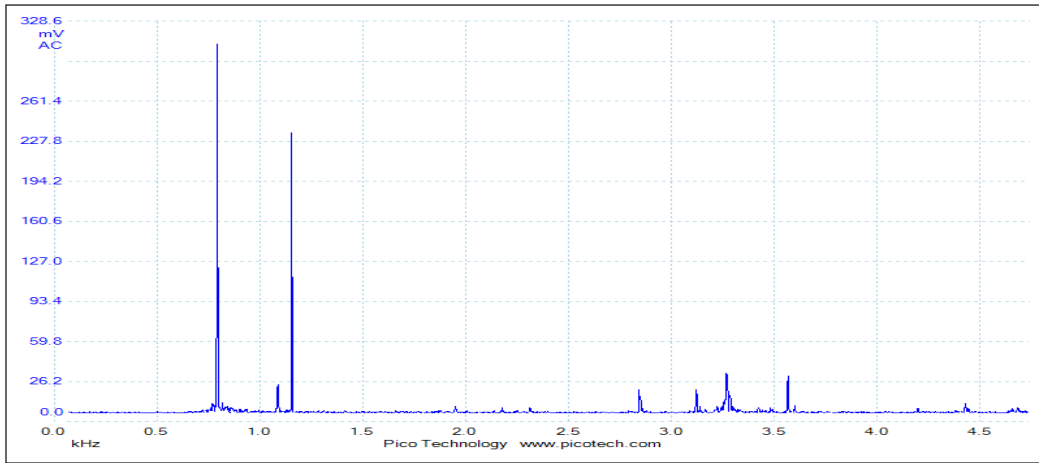
(b)



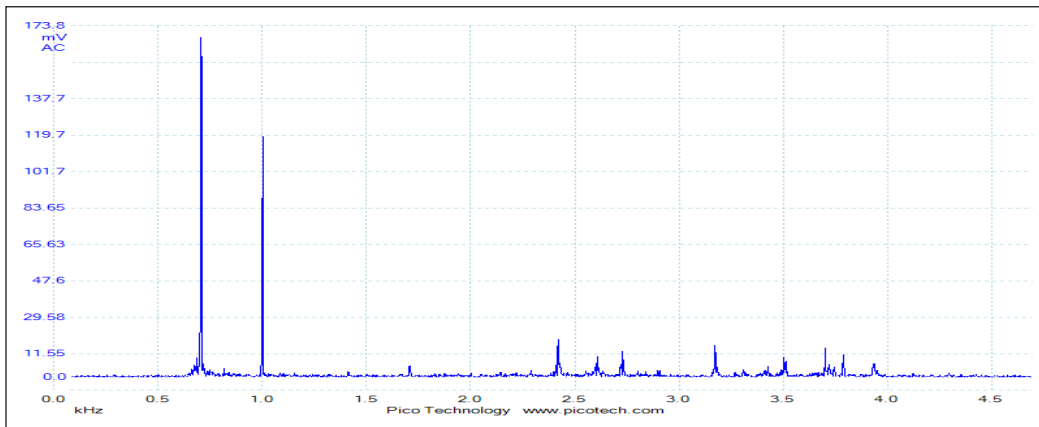
(c)

Figure 7. The acoustic spectra of 8 small gongs of less than 200 mm diameter (label A-H) were recorded about 500 milliseconds after excitation: (a) Gong A; (b) Gong B; and (c) Gong C

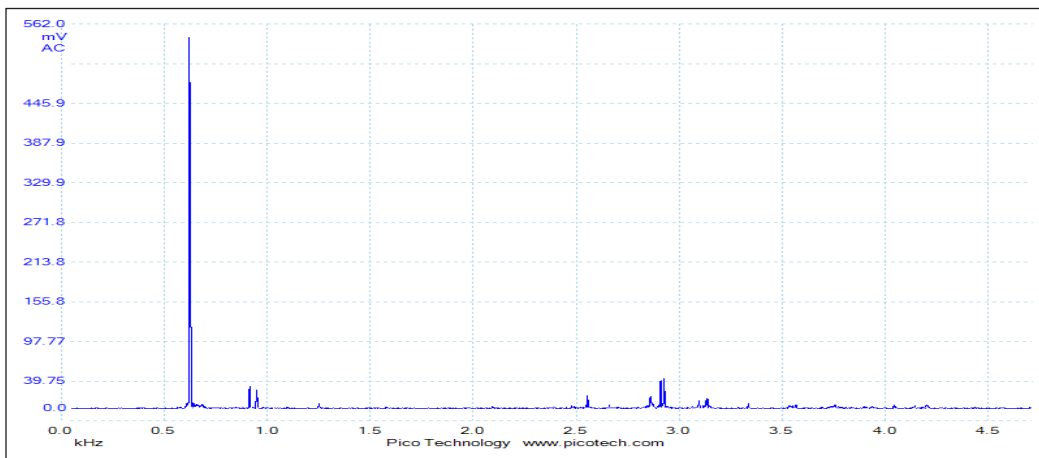
Acoustic and Vibrational Properties of the Kulintang



(d)

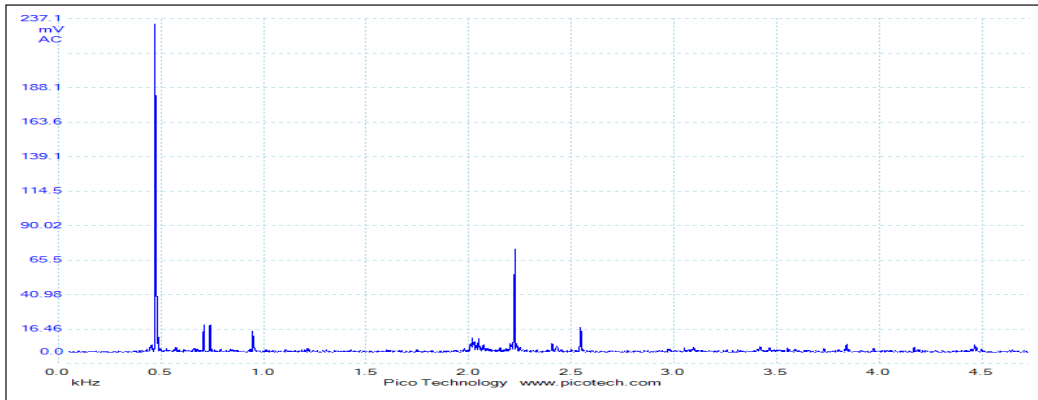


(e)

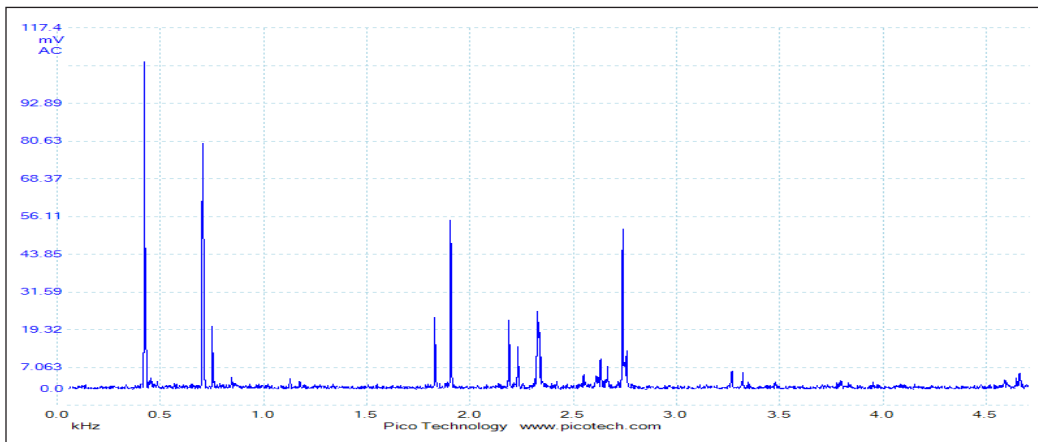


(f)

Figure 7 (continue). The acoustic spectra of 8 small gongs of less than 200 mm diameter (label A-H) were recorded about 500 milliseconds after excitation: (d) Gong D; (e) Gong E; and (f) Gong F



(g)



(h)

Figure 7 (continue). The acoustic spectra of 8 small gongs of less than 200 mm diameter (label A-H) were recorded about 500 milliseconds after excitation: (g) Gong G; and (h) Gong H

of the gong. In Figure 7, we show the gong's time-averaged acoustic power spectrum. It shows that the singlet (0,1) was the most important mode. The (1,1) and (2,2) modes were also significant. It is proven in Table 2 in the ESPI experiment. Only  $n=1$  modes and some of their (non-linear) harmonics made worthwhile contributions. No evidence of a second important axisymmetric mode, as reported by Rossing using a different small gong, was found. Rossing may have observed a harmonic or a subharmonic of the (0,1). In the present ESPI experiments, a true (0,1) mode was found at 1055 Hz (gong B), 624 Hz (gong F), and 474 Hz (gong G).

### Laser Doppler Vibrometer (LDV)

By identifying the resonance frequencies, the gong was subjected to harmonic excitation while keeping the excitation frequency constant and increasing the amplitude; a Laser

Doppler vibrometer (LDV) captured the vibration of the Eigen frequency from the gong. The spectra showed that all resonant peaks are extremely sharp. Some peaks did not correspond to any modes detected by ESPI. These enabled gaps in the overall mode data to be filled, although their nodal patterns had to be inferred.

The frequency obtained using LDV and ESPI measurements are shown in Tables 1 and 2, respectively. Data above 5 kHz had been excluded due to difficulty interpreting their ESPI forms. Such a deviation is caused by variations in the thickness of the gong during casting. Table 1 shows the Eigen frequency with the Eigen number for all series of gongs obtained from the LDV.

Table 1  
Eigen number with Eigen frequency (Hz) for all series of gongs obtain from the LDV

Eigen number	1	2	3	4	5	6	7	8	9	10	11	12
A	1240	1621	3954	4484	-	-	-	-	-	-	-	-
B	1055	1400	3143	3253	3442	3795	4061	4224	4491	4642	-	-
C	934	1317	2584	2858	2994	3299	3675	3943	4251	-	-	-
D	792	1155	1949	2177	2311	2843	3119	3267	3564	-	-	-
E	705	1000	1708	2419	2607	2727	2897	3170	3503	3703	3786	4856
F	624	915	1251	2552	2911	3097	3334	3534	3753	4045	4197	4827
G	474	708	950	2018	2225	2406	2545	3050	3420	3466	3841	4168
H	422	704	1904	2188	2325	2632	2739	3264	4662	-	-	-

Figure 8 shows the typical progressive decay from the gong at a specific Eigen frequency using LDV. The Eigen frequency versus Eigen number for all series of gongs obtained from the LDV is shown in Figure 9.

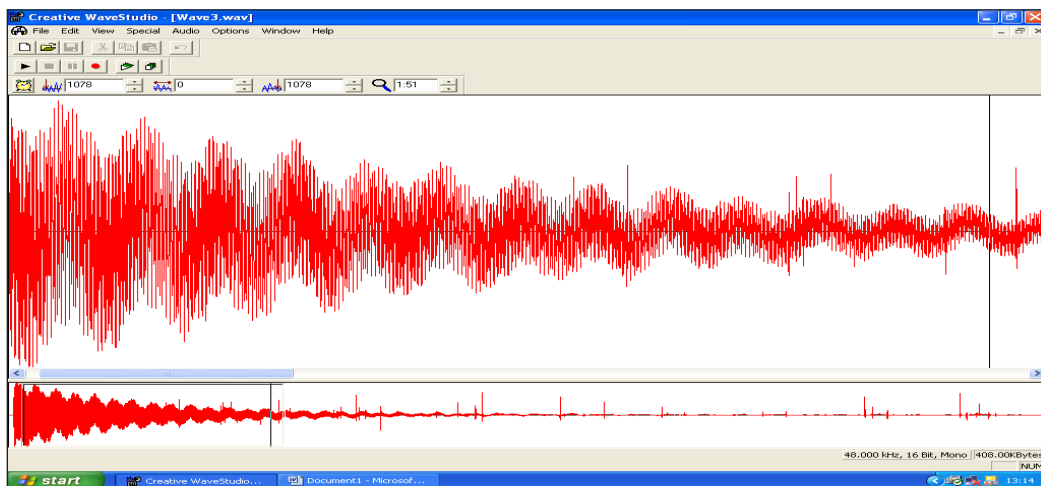


Figure 8. Decay signal from the gong at a specific Eigen frequency using LDV

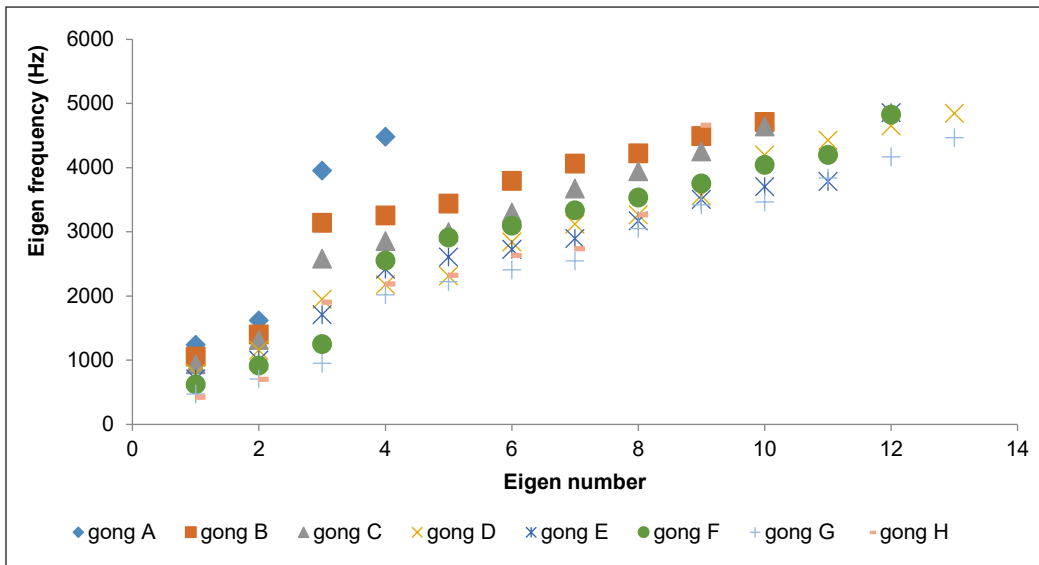


Figure 9. Eigen frequency versus Eigen number for all series of the gong from the LDV

### Electronic Speckle Pattern Interferometry (ESPI)

The operational deflection shapes were studied using Electronic Speckle Pattern Interferometry ESPI. The patterns of the vibration from ESPI are shown in Figure 10. The frequencies and frequency ratio (bold number indicates near harmonic) of the modes (obtained from the ESPI) for all small gongs are given in Table 2.

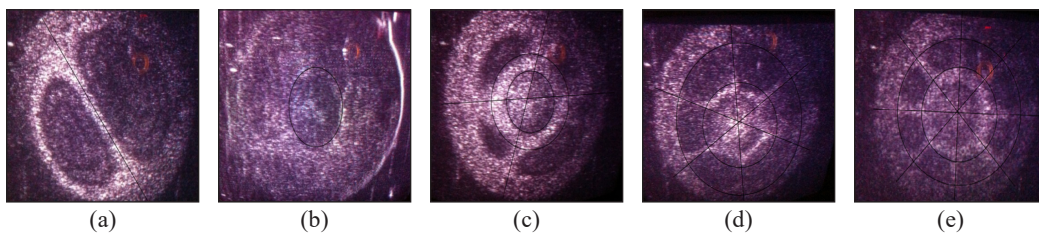


Figure 10. The patterns of the vibration from ESPI: (a) (1,1) from all gongs; (b) (0,1) from Gong B, (1055), F (624), and G (474) Hz; (c) (2, 2) from Gong B (3143), D (2311), E (2607), F (2544), and H (1904) Hz; (d) (3, 2) from Gong C (3299), D (3119), F (2911), G (2018), and H (2188) Hz; and (e) (4, 2) from Gong C (3675) and E (3170) Hz

The notation (m, n) represented a mode with ‘m’ nodal diameters and ‘n’ nodal circles. The approximate ESPI suggested that the fundamental peak at 1055 Hz (gong B), 624 Hz (gong F), and 474 Hz (gong G) is the (0, 1) mode. From Table 2, all gongs display the (1, 1) mode at 1621 Hz (A), 1400 Hz (B), 1317 Hz (C), 1155 Hz (D), 1000 Hz (E), 915 Hz (F), 788 Hz (G) and 701 Hz (H). The strong modes at 3143 Hz (harmonic ratio 3:1 for gong B) are the (2, 2) mode, at 3675 Hz (harmonic ratio 4:1 for gong C) is the (4, 2)

Table 2

Prominent partials in the sound measured acoustically obtained from LDV and (m, n) obtained from ESPI

<b>Gong A</b> <b>(17 cm)</b>	<b>Freq (Hz)</b>	<b>1240</b>	<b>1621</b>	<b>3954</b>	<b>4484</b>	---	---	---	---	---	---
	Freq ratio	1	1.30	<b>3.19</b>	3.62	---	---	---	---	---	---
	Mode(m,n)	---	(1,1)	---	---	---	---	---	---	---	---
<b>Gong B</b> <b>(17.6 cm)</b>	<b>Freq (Hz)</b>	1055	1400	3143	3253	3442	3795	4061	4224	---	---
	Freq ratio	1	1.33	<b>2.98</b>	<b>3.08</b>	3.26	3.6	3.85	<b>4.00</b>	---	---
	Mode(m,n)	(0,1)	(1,1)	(2,2)	---	---	---	---	---	---	---
<b>Gong C</b> <b>(17.8 cm)</b>	<b>Freq (Hz)</b>	934	1317	2548	2858	2994	3299	3675	3943	4251	4642
	Freq ratio	1	1.41	2.77	<b>3.06</b>	3.21	3.53	<b>3.93</b>	4.22	4.55	<b>4.97</b>
	Mode(m,n)	---	(1,1)	---	---	---	(3,2)	(4,2)	---	---	---
<b>Gong D</b> <b>(17.8 cm)</b>	<b>Freq (Hz)</b>	792	1155	1949	2177	2311	2843	3119	3267	3564	4197
	Freq ratio	1	1.46	2.46	2.74	<b>2.91</b>	3.59	<b>3.94</b>	4.13	4.5	5.30
	Mode(m,n)	---	(1,1)	---	---	(2,2)	(2,2)	(3,2)	---	---	---
<b>Gong E</b> <b>(18.2 cm)</b>	<b>Freq (Hz)</b>	705	1000	1708	2419	2607	2727	2897	3170	3503	3703
	Freq ratio	1	1.42	2.42	3.43	3.69	3.86	4.11	4.50	<b>4.97</b>	5.25
	Mode(m,n)	---	(1,1)	---	---	(2,2)	---	---	(4,2)	---	---
<b>Gong F</b> <b>(19 cm)</b>	<b>Freq (Hz)</b>	624	915	1251	2554	2911	3097	3334	3534	3753	4045
	Freq ratio	1	1.47	<b>2.00</b>	4.09	4.67	4.96	5.34	5.66	<b>6.01</b>	6.48
	Mode(m,n)	(0,1)	(1,1)	(1,2)	(2,2)	(3,2)	---	---	---	---	---
<b>Gong G</b> <b>(20 cm)</b>	<b>Freq (Hz)</b>	474	708	950	2018	2225	2406	2545	3050	3420	3466
	Freq ratio	1	1.49	<b>2.00</b>	4.26	4.69	<b>5.08</b>	5.37	6.43	7.22	7.31
	Mode(m,n)	(0,1)	(1,1)	---	(3,2)	---	---	---	---	---	---
<b>Gong H</b> <b>(18.6 cm)</b>	<b>Freq (Hz)</b>	422	704	1904	2188	2325	2632	2739	3264	4662	---
	Freq ratio	1	1.67	4.51	5.18	5.51	6.24	6.49	7.73	11.1	---
	Mode(m,n)	---	(1,1)	(2,2)	(3,2)	---	---	---	---	---	---

mode, at 2311 Hz and 3119 Hz (harmonic ratio 3:1 and 4:1 for gong D) is the (2, 2) and (3, 2) mode, at 2607 Hz, and 3170 Hz (non-harmonic ratio 3.69 and 4.50 for gong E) is the (2, 2) and (4, 2) mode, at 1251 Hz, and 2554 Hz (harmonic ratio 2:1 and 4:1 for gong F) is the (1, 2) and (2, 2) mode, at 2018 Hz (non-harmonic ratio 4.26 for gong G) is the (3, 2) mode, at 1904 Hz and 2188 Hz (non-harmonic ratio 4.51 and 5.18 for gong H) is the (2, 2) and (3, 2) mode. The finding of this research shows that the mode of vibration for each gong may be the (1, 1) mode (Table 2). Mode (0, 1) appears for B, F, and G gongs. Mode (2, 2) appears for B, D, F, E, and H gongs. Mode (3, 2) appears for C, D, F, G, and H gongs. Mode (4, 2) appears for C and E gongs. Issues with the above images must be discussed before meaningful evaluation can begin. Noticeably, there appear to be repetitions of mode shapes, i.e., (2, 2) for gong D at 2311 and 2843 Hz. It is not simply the opposing member of a degenerate pair but repetitions of the mode shapes and nodal line locations. These modes (2, 2) appear and can therefore be denoted as sub-harmonics or harmonics,

respectively (at frequency ratios of 2.91 and 3.59). A prime example of this phenomenon is in Figure 10 is shown for gong D at 2311 Hz.

In Figure 10, harmonic relationships can be found for the (0, 1) modes for gong B at 1055 Hz, gong F at 624 Hz, and gong G at 474 Hz at a frequency ratio of 1 (octave). For gong B and C, harmonic relationships can also be found for the (2, 2) modes (at 3142 Hz at a frequency ratio of 2.98) and (4, 2) modes (at 3675 Hz at a frequency ratio of 3.93), respectively. Two harmonic relationships can also be found for the (2, 2) and (3, 2) modes for gong D (at 2311 and 3119 Hz, respectively, at frequencies ratio of 2.91 and 3.94, respectively). Harmonic relationships for gong F and H can also be found for the (2, 2) modes (at 2554 Hz at a frequency ratio of 4.09) and (3, 2) modes (at 2188 Hz at a frequency ratio of 5.18), respectively. This phenomenon can represent a difficulty in mode classification, as the modes are visible at more than one frequency ratio and could be different for different gongs where the mode for a harmonic relationship can be one only or two.

The frequencies observed in ESPI are real results forced through acoustic excitations. The Eigen frequencies in LDV are obtained from the resonance frequency through the microphone method. LDV, however, only simply showed the Eigen frequencies, but not the vibration mode of the gong. It is, therefore, not surprising that these two sets of frequencies, LDV and ESPI, do not complement each other. The modes from the ESPI images were much more difficult to identify. The gong has significant non-linear properties, as shown by both harmonics and subharmonics of many true modes and some mixed-symmetry types. With  $n \geq 2$ , some serious pattern distortions occur.  $n=1$  was relatively easy to identify because their single nodal circle occurred at or near the inner edge of the shoulder.

In Figure 10, it is clearly visible that the modes are not perfectly formed. There is a large evanescent area to the top right of the gong in the lower-frequency images, and in the higher-frequency images, the nodes are not fully formed and of equal size. These imperfections in the nodal shapes could be caused due to an asymmetry in the gong or perhaps between the gong and the clamp used to hold the gong in place during experiments.

In the above mode shape, there are more partially formed modes than would be expected from a well-produced symmetric gong, and as such, the classification of the modes became arduous. The (4, 2) mode is a possible example of symmetry causing mode shapes to become uniform. A previously mentioned difficulty is the challenge of correctly denoting nodal patterns. The acoustical radiation is produced by motion normal to the surface. The modes are described in terms of the nodal patterns of their radial components.

Due to its axial symmetry, a perfect gong is subject to the same consequences for its normal modes as are other systems with the symmetry group  $C$ , such as bells, cymbals, and at circular plates.  $(m, n)$  can be used to specify a degenerate pair of modes of a particular physical type. However, there are always imperfections in both geometry and metallurgy

since the gongs are cast or formed. These imperfections caused the doublets to be split and the locations of their nodal diameters to be fixed. The gong deviated considerably from perfect axial symmetry causing significant distortions in some of the nodal patterns.

## CONCLUSION

The small gong A-H has an approximately harmonic spectrum with a fundamental frequency of 1240, 1055, 934, 792, 705, 624, 474, and 422 Hz. Gong A with third harmonic (3.19) at 3954 Hz. Gong B with third harmonics (2.98 and 3.08) at 3143 and 3252 Hz and fourth harmonic (4.00) at 4224 Hz. Gong C with third (3.06), fourth (3.93), and fifth harmonics (4.97) at 2858, 3675, and 4642 Hz, respectively. Gong D with third (2.91) and fourth (3.94) harmonics at 2311 and 3119 Hz, respectively. Gong E with fifth harmonics (4.97) at 3503 Hz. Gong F with the second (2.00) and sixth (6.01) harmonics at 1251 and 3753 Hz, respectively. Gong G with the second (2.00) and fifth (5.08) harmonics at 950 and 2406 Hz, respectively. Gong H did not show any harmonics at all.

In this paper, a method to visualise the vibrational mode of kulintangan has been discussed. It is possible to view the type of the mode. It was found that kulintangan may be vibrated at (0, 1), (1, 1), (2, 2), (3, 2), and (4, 2) modes with free edge conditions. The pattern of the vibration can be seen from the ESPI. This finding can be a starting point for further research on the vibrational mode of kulintangan.

## ACKNOWLEDGEMENTS

The authors are grateful to Universiti Malaysia Sarawak for the financial and technical support.

## REFERENCES

- Alman, J. H. (1961). If you can sing, you can beat a Gong. *Sabah Society Journal*, 2, 29-41.
- Dayou J. (2002, July 15-18). *A method to determine the quality of sound from a Kulintangan Set*. [Paper presentation]. Borneo Research Council Seventh Biennial International Conference, Kota Kinabalu, Sabah.
- Batahong, R. Y. & Dayou, J. (2003, March 18-19). Visualizing the vibrational modes of Kulintangan. [Paper Presentation]. National Postgraduate Seminar, Kota Kinabalu, Sabah, Malaysia. [https://www.researchgate.net/publication/339391008\\_VISUALIZING\\_THE\\_VIBRATIONAL\\_MODES\\_OF\\_KULINTANGAN](https://www.researchgate.net/publication/339391008_VISUALIZING_THE_VIBRATIONAL_MODES_OF_KULINTANGAN)
- Dusin, L. (2001). Pengukuran frekuensi bunyi Gong menggunakan kaedah transformasi fourier [Gong sound frequency measurement using Fourier transformation method] [Bachelor thesis]. Universiti Malaysia Sabah, Malaysia. [https://books.google.com.my/books/about/Pengukuran\\_frekuensi\\_bunyi\\_gong\\_mengguna.html?id=i0LItQEACAAJ&redir\\_esc=y](https://books.google.com.my/books/about/Pengukuran_frekuensi_bunyi_gong_mengguna.html?id=i0LItQEACAAJ&redir_esc=y)
- Fletcher, N. H., & Rossing, T. D. (1998). *The physics of musical instruments* (2nd ed.). Springer.

- Frame, E. M. (1976). Several major musical forms of Sabah, Malaysia. *Journal of the Malaysian Branch of the Royal Asiatic Society*, 49(230), 156-163.
- Herington, N., Elford, D. P., Swallowe, G. M., Chalmers, L., Perrin, R., & Moore, T. R. (2010, September 15-18). *Normal modes of a Gamelan Gong*. [Paper presentation]. 1st EAA EuroRegio: Congress on Sound and Vibration, Ljubljana, Slovenia.
- McLachlan, N. (1997). Finite element analysis and gong acoustics. *Acoustics Australia*, 25(3), 103-108.
- Perrin, R., Elford, D. P., Chalmers, L., Swallowe, G. M., Moore, T. R., Hamdan, S., & Halkon, B. J. (2014). Normal modes of a small gamelan gong. *The Journal of the Acoustical Society of America*, 136(4), 1942-1950. <https://doi.org/10.1121/1.4895683>.
- Raman, C.V. (1934). The Indian musical drums. *Proceedings of the Indian Academy of Sciences - Section A*, 1(3), 179-188. <https://doi.org/10.1007/BF03035705>.
- Schneider, A. (2001). Sound, pitch, and scale: From "tone measurements" to sonological analysis in ethnomusicology. *Ethnomusicology*, 45(3), 489-519. <https://doi.org/10.2307/852868>